

Predicting The Occurrence Of Mixed Mode Failure During Hydraulic Fracturing

Robert Charles Choens; Texas A&M University; Ph.D. Candidate; Geophysics, 2015
Manager: Moo Lee; Mentor: Steve Bauer; Geoscience, Climate, and Consequence Effect; 6913
Sandia National Laboratories/NM, U.S. Department of Energy
July 31, 2014

Abstract:

Axisymmetric triaxial extension experiments were performed on Berea sandstone, Carrara marble, and Indiana limestone to investigate localization behavior in the transition from tensile to shear failure. Samples were instrumented with strain gages that were able to capture the mechanical behavior as localized failure began. The geometry of the samples allows the rock to fracture with minimal stress concentrations effects, producing a gradual change in angle as the confining pressure is increased from extension to shear. The fracture angles and failure strengths reported are inconsistent with predictions from the Griffith and modified Griffith criteria.

The strain gage data was used to compare the experimental results against predictions for localization from constitutive models based on bifurcation theory. The classic model derived from Rudnicki and Rice (1975) are not able to predict the experimental results. Later derivations that allowed for multiple yield surface models from Challa and Issen (2004) are not better able to predict the expected failure type or fracture orientation. The constitutive model based off three stress invariants from Rudnicki (2008) has the most accurate predictions of fracture angles out of the models based on bifurcation theory. The inability of the constitutive models to predict the failure type and orientation reflect the difficulty in capturing the changing mechanisms from tensile to shear failure.

Method

Details of experiments

The triaxial extension experiments presented here employ the notch-cut, or 'dogbone,' sample geometry employed in the studies by Ramsey and Bobich (Figure 1) which allows the confining pressure to generate an axial tensile stress and radial compressive stress in the center of the sample. The samples will be instrumented with orthogonal strain gages in the necked region to measure the axial and radial strain components in the failure region during loading. Previous experiments depended on axial strain measured over the entire sample length and did not measure radial strain, therefore these experiments could not calculate the elastic moduli or other key parameters for bifurcation analysis. The axial and radial strain measurements will demonstrate how the moduli evolve through the mixed mode transition. The dogbone geometry also offers a great advantage in measuring the strains at failure; the geometry controls the localization point, so the strain gages can be definitively placed to measure the behavior at the onset of failure. In addition to strain measurements, piezoelectric transducers affixed on the sample endcaps will be used to monitor acoustic emissions during deformation. The acoustic emissions measure the amount of microscale fracturing during deformation and can be used to characterize damage evolution through the mixed mode transition.

To create the dogbone geometry, the samples are ground on a microlathe on a stationary surface grinder to create the neck of the sample. The rounded neck of the sample creates a single stress concentration in the center of the neck and reduces the undesirable stress concentrations from the neck – shoulder transition. This rounded geometry allows for greater reproducibility in experimental results. The samples dimensions are 102mm in length, 47mm diameter at the shoulder, and 30mm at the neck with a radius of curvature of 88mm.

A multiple layer jacketing procedure is used to separate the sample from the confining medium. First, a thin latex jacket is used directly next to the sample. Plasticene modeling clay is molded around the sample neck and flush with the shoulders to evenly distribute confining pressure. The sample is isolated from the confining pressure with an outer polyolefin jacket fixed to the piston assembly using nicrome tie wires. The strain gages are affixed to the neck of the sample with epoxy before jacketing. The leads from the gages are connected out of the vessel via a hole in the piston. The sample can be jacketed as described previously.

The samples will be deformed in a triaxial rig with liquid confining media, capable of precise control of the axial piston displacement. The sample is loaded in the vessel and an axial load is applied equal to that of confining pressure. The experimental procedure involves then establishing the confining pressure and backing off the piston until there is a macroscopic stress drop associated with failure. The piston is extended at strain rates of 10-5 per second. Experiments will be performed dry due to permeability constraints. The suite of experiments will start at 10 MPa confining pressure, and increase by 5-10 MPa into the shear failure field. Select extension experiments across the mixed mode transition from Ramsey and Chester, 2004, and Bobich, 2005, will be reproduced with strain gage instrumented samples. This will allow the failure criterion to be correlated to the pre-existing macroscopic and microscopic fracture investigations on Berea sandstone and Carrara marble.

Two suites of experiments are planned:

1) The constitutive behavior suite of experiments will reproduce dogbone extension experiments on Berea sandstone and Carrara marble with strain gage instrumentation to perform bifurcation analysis. The analysis can be combined with previous microstructural analysis to understand and predict the damage accumulation across the mixed mode transition.

2) The material investigation suite of experiments will perform dogbone extension experiments with strain gage instrumentation on a different rock type with markedly different UCS and T0 from Berea sandstone and Carrara marble. This suite of experiments will test the generalized form of the failure envelope and establish the scaling parameters for mechanically different rocks.

Results:

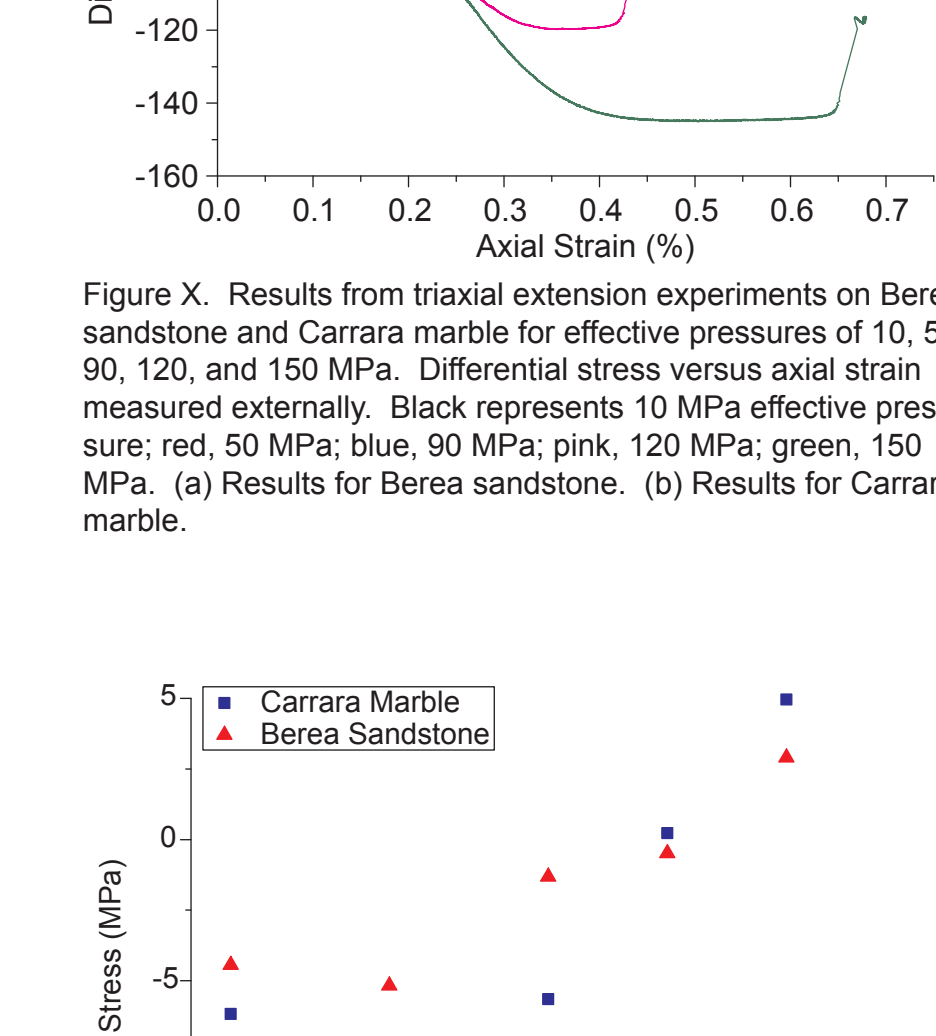


Figure X. Results from triaxial extension experiments on Berea sandstone and Carrara marble for effective pressures of 10, 50, 90, 120, and 150 MPa. Differential stress versus axial strain measured externally. Black represents 10 MPa effective pressure; red, 50 MPa; blue, 90 MPa; pink, 120 MPa; green, 150 MPa. (a) Results for Berea sandstone. (b) Results for Carrara marble.

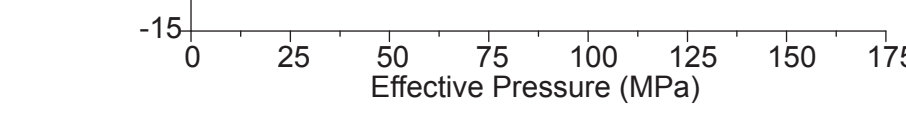


Figure X. Failure strengths for Berea sandstone and Carrara marble in terms of axial stress versus effective pressure. Blue squares represent Carrara marble, red triangles represent Berea sandstone.



Figure X. Changes in fracture angle with pressure. Results from Berea sandstone and Carrara marble plotted in terms of fracture angle versus effective pressure. Blue squares represent Carrara marble, red triangles represent Berea sandstone.



Figure X. Results from Berea sandstone and Carrara marble plotted in terms of differential stress versus mean stress. Blue squares represent Carrara marble, red triangles represent Berea sandstone.

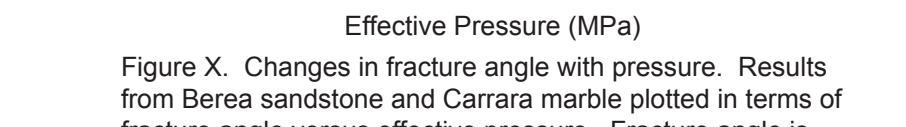


Figure X. Results from Berea sandstone and Carrara marble plotted in terms of square root of stress versus mean stress. Blue squares represent Carrara marble, red triangles represent Berea sandstone.



Figure X. Results from Berea sandstone and Carrara marble plotted in terms of square root of stress versus mean stress. Blue squares represent Carrara marble, red triangles represent Berea sandstone.



Figure X. Results from Berea sandstone and Carrara marble plotted in terms of square root of stress versus mean stress. Blue squares represent Carrara marble, red triangles represent Berea sandstone.

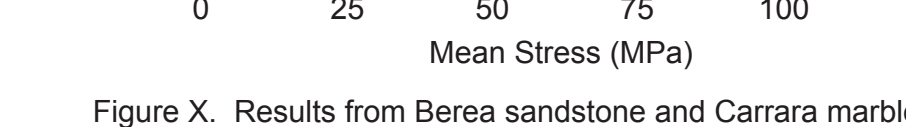


Figure X. Results from Berea sandstone and Carrara marble plotted in terms of square root of stress versus mean stress. Blue squares represent Carrara marble, red triangles represent Berea sandstone.



Figure X. Results from Berea sandstone and Carrara marble plotted in terms of square root of stress versus mean stress. Blue squares represent Carrara marble, red triangles represent Berea sandstone.

Introduction

In recent years, unconventional petroleum reservoirs have had a huge impact on domestic energy production, due in large part to the development of massive hydraulic fracturing in previously uneconomic formations. The induced fracture network enhances the reservoir permeability, allowing production at reasonable rates. The technique has been successful enough to create over a dozen major unconventional plays in the U.S. alone. Because of the rapid proliferation, development has outpaced scientific understanding. Hydraulic fracturing creates tensile fracture in the reservoir, and the behavior of rocks in tension and low mean stresses has been poorly defined. The vast majority of geomechanics research has been focused on the behavior of rocks in compression and shear due to the overwhelmingly compressive states of stress in the Earth. Tensile stresses are usually limited to the very shallow crust where planar joints occur, and deeper in the crust where geothermal, volcanic, or metamorphic processes create an abnormally high fluid pressure that can exceed the minimum principal stress and create complicated hybrid fracture meshes. The tensile strength of rocks can be easily determined, but the behavior with increasing mean stress involves difficult experiments with only a few published values. The standard approach for this type of failure has been to use a theoretical failure criterion that does not match the published experimental results. The failure criterion cannot accurately predict the failure strength, fracture angle, or associated off crack damage seen in experiments like more advanced failure criterion developed for the behavior of rocks in compression.

Hydraulic fracturing is predicted to create planar wing fractures, similar in morphology to joints, and there is evidence from observed fractures that this is the case. There is also evidence that hydraulic fractures do not match this prediction, that the induced network is a large, complicated, interconnected fracture network, more like the fracture meshes seen in geothermal and metamorphic provinces. Complexities in fracturing are often attributed to preexisting fractures, but the similarities to natural examples suggest that a characteristic state of stress at the fracture tip could be causing the complications. Because the production of the unconventional reservoir depends on the permeability of the induced fracture network, it is vital to be able to predict a priori the extent and interconnectivity of the generated fracture network. A thorough understanding of the behavior of rocks in tension and low mean stress based on laboratory experiments is critical to understanding the behavior of hydraulic fractures.

The goal of this study to establish an empirical failure envelope that can be combined with measured parameters to create a theory based constitutive model to predict the failure strength, fracture orientations, and damage evolution of rocks deformed in tension and low mean stress. This study will employ triaxial extension experiments on different materials with novel instrumentation to record plasticity values previously unreported in literature. The objectives of this study are

- Recreate triaxial extension experiments on previous materials with additional instrumentation to develop a constitutive model with predictive capabilities
- Perform suite of triaxial extension experiments on a different strength rock to establish the general form and scaling relationships of the constitutive model
- Combine constitutive model with previous microstructural observations to predict fracture orientations and associated off crack damage
- Combine constitutive model with in situ reservoir properties to predict hydraulic fracture behavior and reactivation potential of preexisting fractures

Figure 1. Sample Assembly.

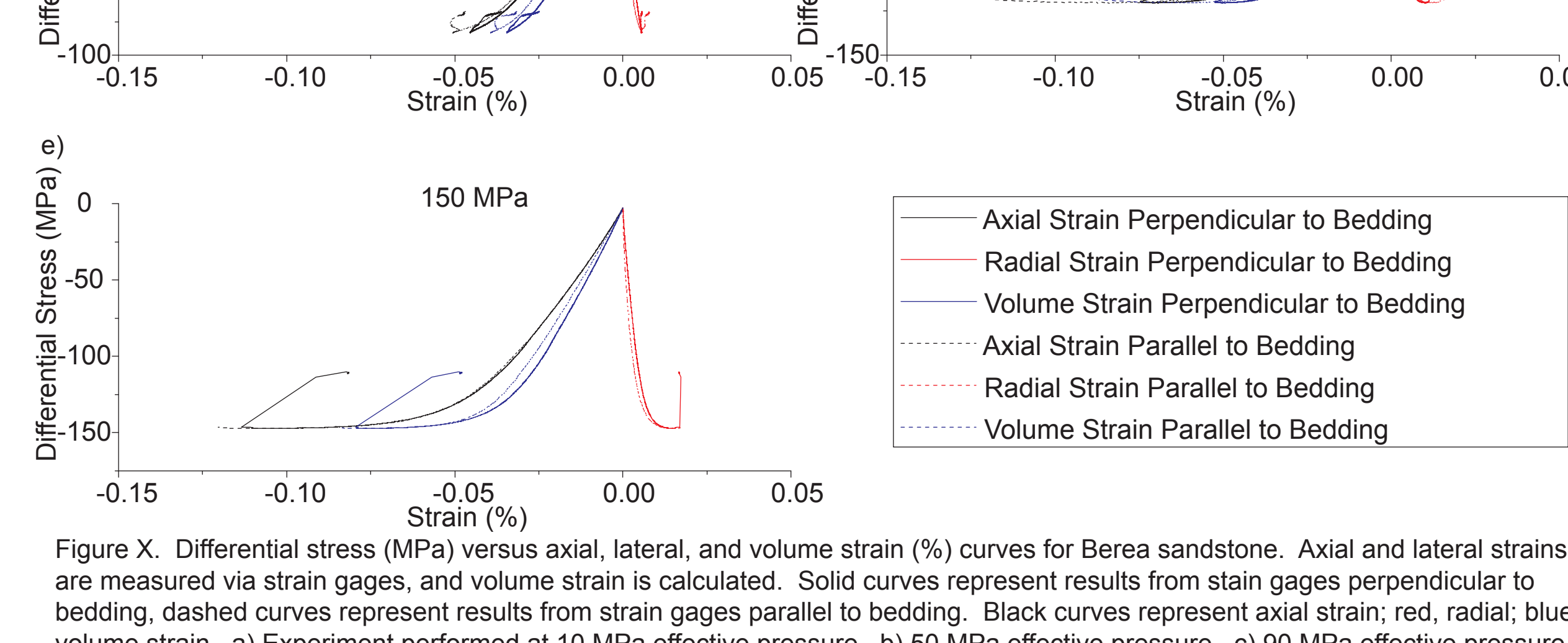
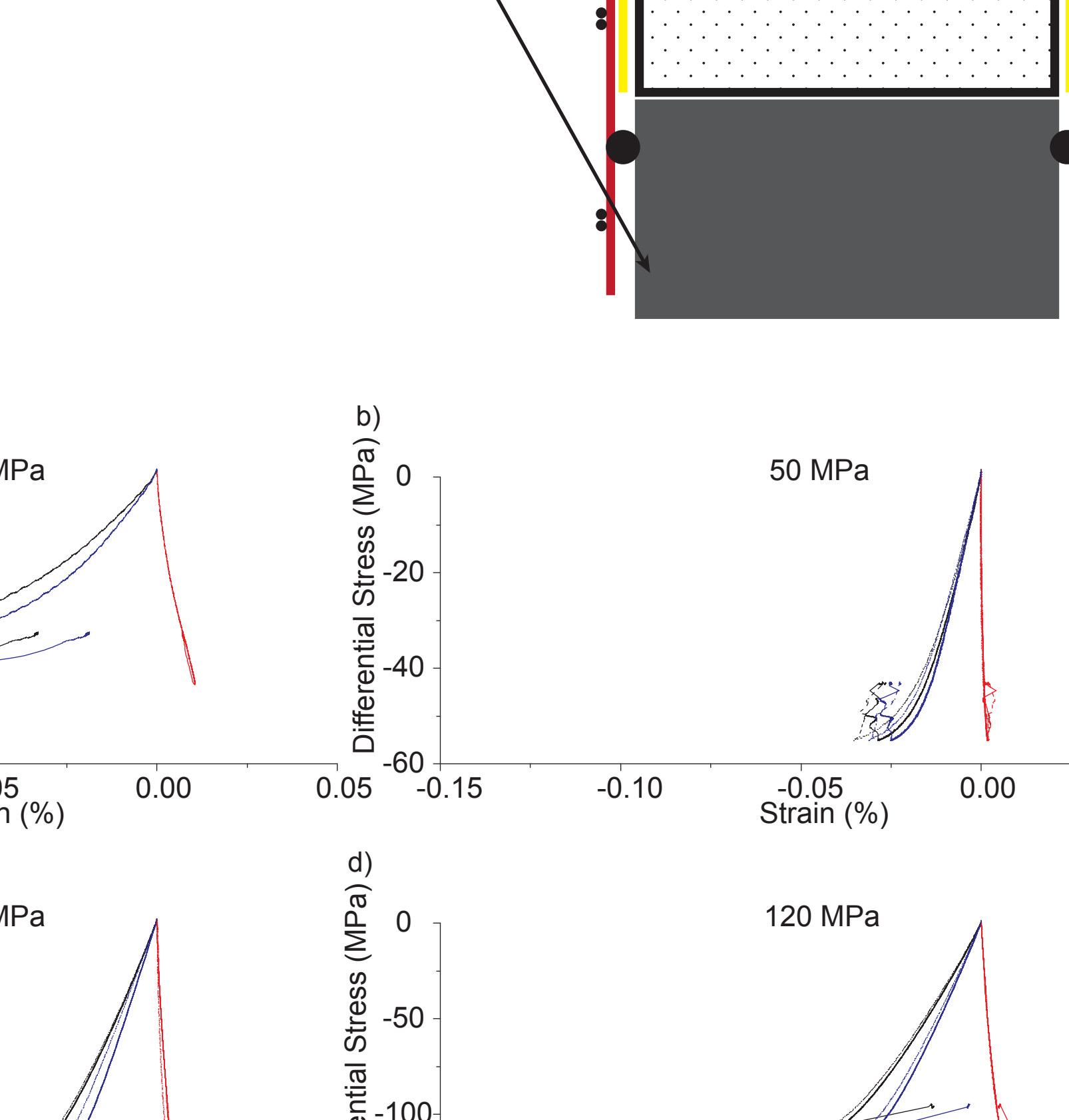


Figure X. Differential stress (MPa) versus axial, lateral, and volume strain (%) curves for Berea sandstone. Axial and lateral strains are measured via strain gages, and volume strain is calculated. Solid curves represent results from strain gages perpendicular to bedding, dashed curves represent results from strain gages parallel to bedding. Black curves represent axial strain; red, radial; blue, volume strain. a) Experiment performed at 10 MPa effective pressure. b) 50 MPa effective pressure. c) 90 MPa effective pressure. d) 120 MPa effective pressure. e) 150 MPa effective pressure.

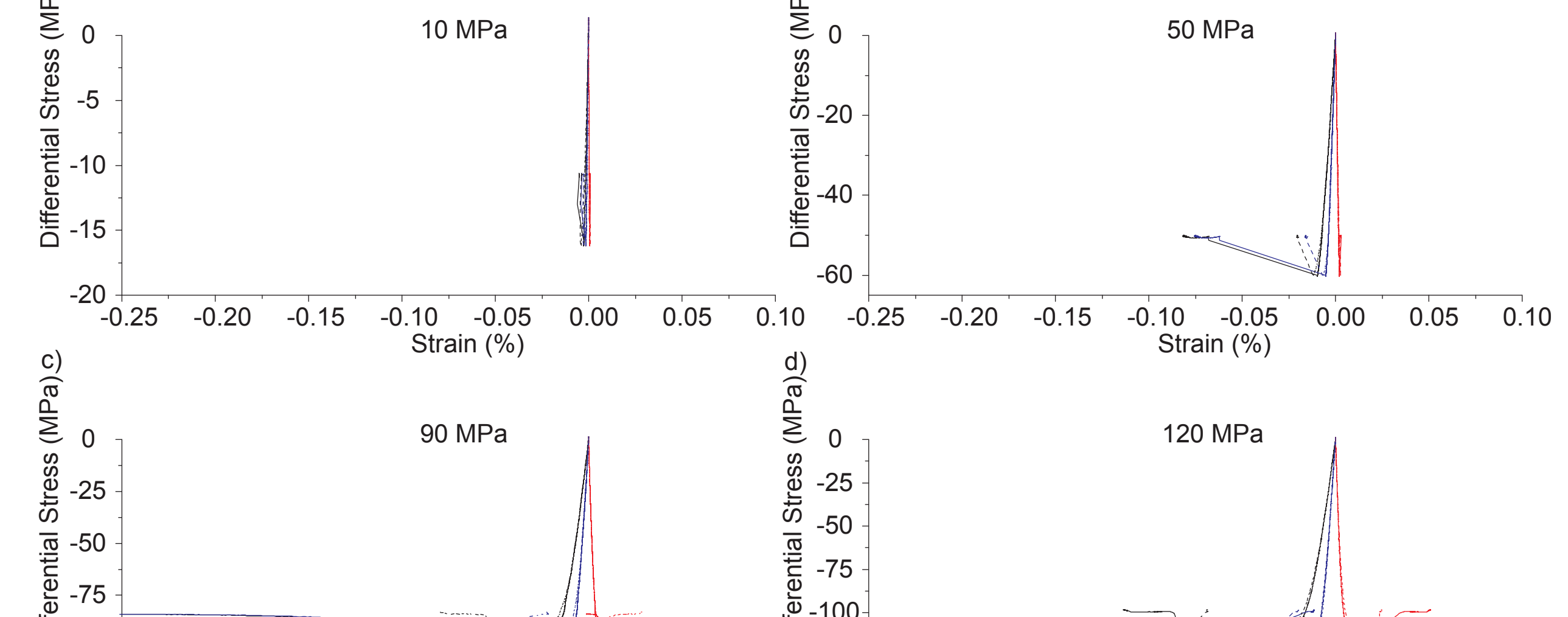


Figure X. Differential stress (MPa) versus axial, lateral, and volume strain (%) curves for Carrara marble. Axial and lateral strains are measured via strain gages, and volume strain is calculated. Solid curves represent results from strain gages parallel to fast P wave velocity, dashed curves represent results from strain gages perpendicular to fast P wave velocity. Black curves represent axial strain; red, radial; blue, volume strain. a) Experiment performed at 10 MPa effective pressure. b) 50 MPa effective pressure. c) 90 MPa effective pressure. d) 120 MPa effective pressure. e) 150 MPa effective pressure.

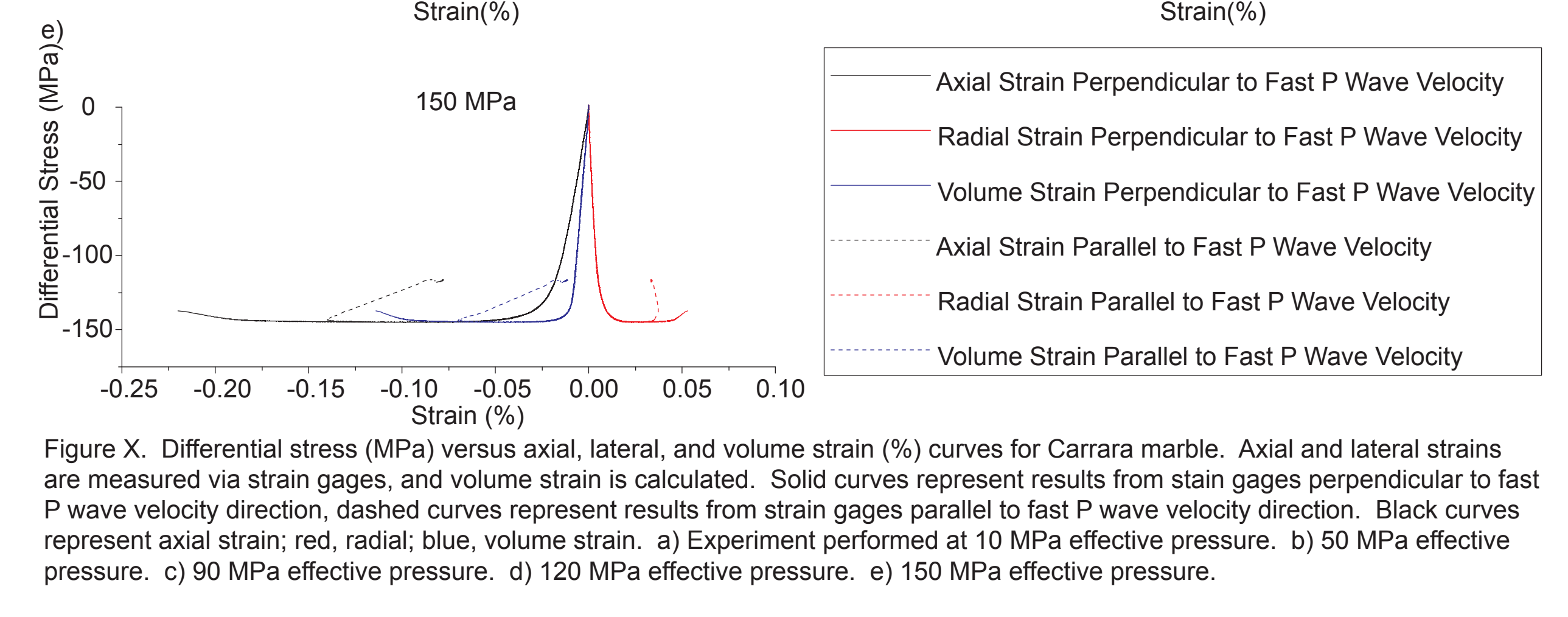


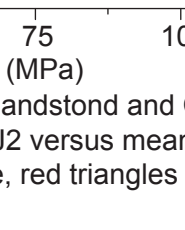
Figure X. Differential stress (MPa) versus axial, lateral, and volume strain (%) curves for Carrara marble. Axial and lateral strains are measured via strain gages, and volume strain is calculated. Solid curves represent results from strain gages parallel to fast P wave velocity, dashed curves represent results from strain gages perpendicular to fast P wave velocity. Black curves represent axial strain; red, radial; blue, volume strain. a) Experiment performed at 10 MPa effective pressure. b) 50 MPa effective pressure. c) 90 MPa effective pressure. d) 120 MPa effective pressure. e) 150 MPa effective pressure.

Discussion:

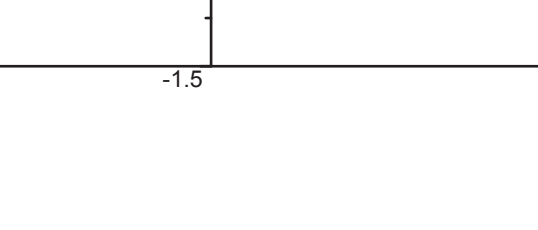
Failure angles and fracture strength match previous work, but do not predict angles.

Mixed mode failure likely to occur in deep reservoirs during hydraulic stimulation.

Investigation into different strength materials ongoing.



Sandia National Laboratories



Sandia National Laboratories is a multi-program laboratory managed and operated by Sandia Corporation for the U.S. Department of Energy. Sandia National Laboratories is a division of Honeywell International Inc., for the U.S. Department of Energy's National Nuclear Security Administration under contract DE-NA0003525. Under contract DE-AC04-94AL85000, the U.S. Department of Energy's